FERMILAB-PUB-78-124-E

Nuclear Interactions of 400 GeV Protons in Emulsion.

I. Otterlund and E. Stenlund,
Dept. of Cosmic and Subatomic Physics,
University of Lund, Lund, Sweden.

B. Andersson and G. Nilsson,
Dept. of Theoretical Physics,
University of Lund, Lund, Sweden.

O. Adamovic and M. Juric,
University of Belgrade, Belgrade, Yugoslavia.

H. Areti, C.J.D. Hébert and J. Hébert,
Université d'Ottawa, Ottawa, Canada.

G. Baumann and R. Devienne,
Université de Nancy, Nancy, France.

J.M. Bolta and M.A. Sanchis,
Universidad de Valencia, Valencia, Spain.

L. Bravo, R. Niembro, A. Ruiz and E. Villar,
Universidad de Santander, Santander, Spain.

C.O. Kim*), J. Lory, C. Meton, D. Schune, Tsai-Chü and B. Willot,
L.P.N.H.E., Université Paris VI, Paris, France.

R. Schmitt,
Laboratoire de Rayonnement Cosmique, Lyon, France.

*) Present address: Korea University, 1. Anam-Dong, Sungbuk-Ku, Seoul, Korea.

We report on 400 GeV proton-emulsion nucleus reactions and compare the results to hadron-nucleus reactions at smaller energies. In particular we present results on the emission of fast target protons (essentially grey track particles) and on their correlation with the number of collisions inside the nucleus, ν, with the number of charged evaporated particles (essentially black track particles) and with the number of pions produced (essentially shower particles). We observe that the main features of the 200-400 GeV data are very similar. However, we find that the mean shower-particle multiplicity at 400 GeV is essentially higher than expected from the simple independent particle model prediction $\langle n_s \rangle = \langle n_{ch} \rangle [1 + 0.5 (\langle \nu \rangle - 1)]$. The shower particle multiplicities do not seem to follow a target mass dependence of the form $\langle n_s \rangle = \langle n_{ch} \rangle A^{\alpha}$ with $\alpha = 0.14$ or $\alpha = 0.19$ as has been suggested in the literature. The pseudo-rapidity distribution shows limiting target and projectile fragmentation. The shower particle multiplicity in the "central region" increases linearily with $\langle \nu \rangle$ but faster than 0.5 $\langle \nu \rangle$ times the corresponding multiplicity in pp-reactions.

1. Introduction.

Hadron-emulsion nucleus (h-Em) reaction studies have principally provided us with results on target fragmentation (multiplicities of singly and multiply charged particles with $\beta < 0.7$, heavy track particles) and pion production (multiplicities and pseudo-rapidity distributions of singly charged particles with $\beta > 0.7$, shower particles). Only in a few investigations have results on the emission of grey-track particles (essentially protons in the energy range 30-400 MeV) been published [1-7]. In this investigation we have evaluated the main features of grey track particles and the results are given in section 2. In section 3 we present a summary of the multiplicities measured within this collabo-

ration at 200, 300 and 400 GeV.

Studies of grey particles are of special interest due to the fact that they are emitted during or shortly after the passage of the leading hadron. We therefore expect them to memorize part of the history of the reaction.

A first attempt to evaluate grey track particle distributions has recently been published [5,7]. B. Andersson et al. [7] have developed a model for high-energy hadron-nucleus reactions which describes how the number of fast target protons, N_g, measure the number of collisions inside the nucleus, ν. This model has been used in section 4 where we evaluate how the shower particle multiplicities depends on $\bar{\nu}(N_g)$.

The limited space-time development of hadronic matter inside a hit nucleus is a probable explanation of the low pion multiplicities in hadron-nucleus reactions and the weak energy dependence of the observables [8,9].

Most comparisons between theory and experimental findings have been concerned with the average multiplicities and only a few attempts have been made to disentangle the multiplicities with respect to the dependence on target mass and incident energy. The necessity of an evaluation of the multiplicities in different fragmentation regions has recently been pointed out by B. Andersson et al. [10]. Thus when we present shower particle rapidity distributions in section 5 we divide them into target and projectile fragmentation regions and a central region. The central region of pseudo-rapidity space is further studied in section 6.

Results from p-A reactions at 400 GeV have been published in

two recent papers. Aggarwal et al. [11] studied the shower particle and heavy prong multiplicities in p-Em reactions. Fumuro et al. [12] used an emulsion chamber to obtain shower particle multiplicities in p-Al, p-Sn, p-Cu and p-W reactions. All the results presented in this paper have been obtained in stacks of Ilford K5, 600 μm emulsions exposed horizontally to the FNAL 400 GeV proton beam. Further details of the experiment can be found in references [6] and [13].

2. Emission of charged target fragments.

The energy independent emission of singly and multiply charged target fragments (heavy track particles) is exemplified in Fig. 1 where we have given the integral distribution of heavy track particles. It is appropriate to divide the charged target fragments into two groups, knock-on recoils (grey track particles) and evaporation particles (black track particles).

Grey track particles (N_g) are mainly protons in the energy range 30-400 MeV. In p-Em reactions at 300-400 GeV they exhibit a differential energy spectrum of the form

$$N(E)dE \sim E^{-\gamma}dE \qquad (1)$$

where N(E) is the number of protons per event and energy unit (MeV). γ has the value 1.09 ± 0.02 [6].

The angular distribution is close to the form

$$\frac{1}{\sigma}\frac{d\sigma}{d(\cos\theta)} \sim \exp(0.96\cos\theta) \qquad (2)$$

and stays constant in the energy range 2-400 GeV (Fig. 2). The forward peaked behaviour supports the assumption that grey particles are knock-on recoils.

Black track particles (N_b) are low energy singly and multiply charged fragments (p,d,t with $E \lesssim 30$ MeV/n and ^{3}He, ^{4}He with $E \lesssim 300$ MeV/n). They are emitted a long time after the passage of the incident hadron ($\sim 10^{-17}$s) and they are mainly evaporation particles. Black track particles exhibit an almost isotropic angular distribution [6].

The dependence of the mean number of black tracks $\langle N_b \rangle$ on N_g is nonlinear and has the same behaviour throughout the energy range 6.2 GeV to 400 GeV. (Fig. 3). For $N_g \gtrsim 10$ a saturation of the $\langle N_b \rangle - N_g$ correlation is reached. The correlation does not depend on the nature of the incident hadron i.e. only the number of recoiling nucleons in the hit nucleus determines the average excitation energy of the residual target nucleus.
The correlation is completely independent of the number of produced pions i.e. the pions do not transfer any significant energy to the target nucleus. Even if the shower particle multiplicity increases from 2.8 (p-A at 6.2 GeV) to 16.8 (p-A at 400 GeV) no change is observed in the mean black track and grey track multiplicities.

It has often been suggested that the number of grey prong particles, N_g, is a measure of the number of encounters, ν, between the incident hadron and the target nucleons. This suggestion has been strongly supported by the results presented in two recently published papers where a relationship is obtained between the number of fast target protons (grey-prong producing particles) and the number of collisions of the impinging hadron inside the nucleus [5,7].

The N_g-distribution in p-A reactions, $P_A(N_g)$, according to the model suggested by Andersson et al. [7], is

$$P_A(N_g) = \sum_\nu \pi_A(\nu) P_\nu^A(N_g) \qquad \text{where} \qquad (3)$$

$$P_\nu^A(N_g) = \binom{N_g+\nu-1}{N_g} (1-X)^\nu X^{N_g} \qquad \text{and} \qquad (4)$$

$$X = \frac{\langle N_g \rangle}{\langle \nu \rangle} \left(1 + \frac{\langle N_g \rangle}{\langle \nu \rangle}\right)^{-1} = 0.35 \text{ for CNO and } 0.54 \text{ for AgBr.}$$

The probability $\pi_A(\nu)$, that the incident hadron h collides ν times in the nucleus A, is in our investigation taken from a Monte Carlo calculation with a Woods-Saxon nuclear density distribution [21].

The dotted curve in Fig. 4, predicted from eq. (3), is close to the observed distributions. The small disagreement for $N_g = 1$ can be explained by contributions from pp-reactions.

In chapters 4 and 6 we study the shower particle multiplicities as a function of $\bar{\nu}(N_g)$. The $\bar{\nu}(N_g)$-values

$$\bar{\nu}(N_g) = \frac{\sum_\nu \nu \pi_{h,A}(\nu)\ P_\nu^A(N_g)}{\sum_\nu \pi_{h,A}(\nu)\ P_\nu^A(N_g)} \qquad (5)$$

have been estimated using eq. (4).

4. Emission of shower particles.

In Fig. 5 we present the scaled multiplicity distribution in reactions at 67-400 GeV. The multiplicity values differ slightly from the scaled distribution computed from the Slattery pp-distribution [22] summed over the different constituents of the target (dashed curve in Fig. 5).

In Figs. 6-8 we exhibit some features of the correlations between the shower particles and the heavy track particles in the range 200-400 GeV. In Fig. 6 the mean value $\langle R \rangle = \frac{\langle n_s \rangle}{\langle n_{ch} \rangle - 0.5} = \frac{\langle n_s \rangle}{\langle n_s \rangle_p}$ is plotted for different values of N_h, and in Fig. 7 we exhibit the correlation between $\langle N_h \rangle$ and R. $\langle n_{ch} \rangle$ is the

mean charged particle multiplicity in pp-reactions.

$\langle n_s \rangle_p = \langle n_{ch} \rangle - 0.5$ is approximately the shower particle multiplicity in a proton-nucleon collision [23] . Fig. 8 shows $\langle n_s \rangle / D$ as a function of N_h.

From Figs. 5-8 we conclude that the mean features of the 200, 300 and 400 GeV data are very similar. In particular the close correlation between shower particles and target nucleus fragmentation is noticeable. The constancy of $\langle N_h \rangle$ for values of $R < 1$ and the increase of $\langle N_h \rangle$ for $R > 1$ is obvious. $\langle n_s \rangle / D$ increases with N_h, a feature which is expected from the independent particle model.

It is appropriate to disentangle the total shower particle multiplicity $\langle n_s \rangle$ into contributions from different processes and different targets. For p-Em reactions we obtain:

$$k \langle n_s \rangle = \langle n_s \rangle_H \cdot 0.04 + \langle n_s \rangle_{CNO} \cdot 0.25 + \langle n_s \rangle_{AgBr} \cdot 0.71$$

k is a correction for coherently produced shower particles. $\langle n_s \rangle_H = \langle n_{ch} \rangle - 0.5$ is the shower particle multiplicity in proton-proton reactions [23] , $\langle n_s \rangle_{CNO}$ and $\langle n_s \rangle_{AgBr}$ are the multiplicities in incoherent reactions in CNO and AgBr, respectively. The incoherent shower particle multiplicities in CNO and AgBr is then given by the equation:

$$\langle n_s \rangle_i = 0.26 \langle n_s \rangle_{CNO} + 0.74 \langle n_s \rangle_{AgBr} = [k \langle n_s \rangle - 0.04 \langle n_s \rangle_H] \, 1.04$$

A k value equal to 1.03 has been used in the range 200-400 GeV [2,14,15]. At energies < 70 GeV we have not considered any coherent production and have therefore k = 1.

We shall here compare our measured multiplicities to the independent particle model prediction

$$\langle n_s \rangle_i = \langle n_o \rangle + \langle n_i \rangle \langle \nu \rangle \qquad (6)$$

$\langle n_o \rangle$ is the "leading particle multiplicity" and $\langle n_1 \rangle$ is interpreted as the average number of particles produced in each of the collisions inside the nucleus. $\langle \nu \rangle$ is the number of encounters between the incident hadron and the target nucleons.

It has been suggested in the literature [23,24] that the shower particle multiplicity should be given by the equation

$$\langle n_s \rangle_i = \frac{\langle n_{ch} \rangle}{2} (1 + \langle \nu \rangle), \tag{7}$$

where the number of collisions $\langle \nu \rangle$ is defined by the equation

$$\langle \nu \rangle = \frac{A \cdot \sigma_{hp}}{\sigma_{hA}} \quad . \tag{8}$$

σ_{hp} and σ_{hA} are the inelastic cross sections for hadron-proton and hadron-nucleus interactions, respectively.

This model thus predicts $\langle n_o \rangle = \langle n_1 \rangle = \frac{1}{2} \langle n_{ch} \rangle$ in eq. (6). To compare the predictions from eq. (7) with our experimental findings we show in Fig. 9 the energy dependence of

$$\langle n_1 \rangle = \frac{\langle n_s \rangle_i - \frac{\langle n_{ch} \rangle}{2}}{\langle \nu \rangle} \tag{9}$$

(i.e. the number of shower particles which on the average are produced in the collisions inside the nucleus, if we assume that the "leading particle multiplicity" is $\frac{\langle n_{ch} \rangle}{2}$).

The close agreement between p-E_m and π-E_m data in Fig. 9 shows that $\langle n_1 \rangle$ is independent of the nature of the incident hadron. The solid curve shows $\langle n_1 \rangle = \frac{1}{2} \langle n_{ch} \rangle$. In the range 100-200 GeV this formula gives approximately the experimentally measured multiplicities. However, for both higher and lower energies the discrepancy is considerable.

In table 1 we compare experimental multiplicities in the energy range 6-400 GeV with the theoretical predictions $\langle n_{ch}\rangle[1+\frac{1}{2}(\langle\nu\rangle-1)]$, $\langle n_{ch}\rangle\cdot A^{.14}$ and $\langle n_{ch}\rangle\cdot A^{.19}$ and we conclude that the multiplicity at 400 GeV is not in agreement with any of the models.

The dependence of the shower particle multiplicity on N_g is shown in Fig. 10. A linear behaviour is observed for small values of N_g. However, already for N_g-values around 5, deviations occur. A linear dependence is obtained when $\langle n_s\rangle$ is plotted as a function of the quantity $\bar{\nu}(N_g)$ defined by eq. (5) (Fig. 11). The emulsion results follow the equation

$$\langle n_s\rangle = (3.1 \pm 0.8) + (5.5 \pm 0.2)\ \bar{\nu}(N_g) \qquad (10)$$

For $\nu=1$ equation (10) gives $\langle n_s\rangle = 8.6 \pm 0.6$, which is close to the value $\langle n_{ch}\rangle = 8.99 \pm 0.14$ from pp-reactions [27]. $\langle n_s\rangle = 5.5 \pm 0.2$ is larger than $\frac{1}{2}\langle n_{ch}\rangle$ and close to the multiplicity value at 400 GeV shown in Fig. 9.

Fumuro et al. [12] have measured multiplicities in proton reactions with Al, Cu, Sn and W at 400 GeV using an emulsion chamber in which metallic foils of Al, Cu, Sn and W were sandwiched in nuclear emulsion. The target nucleus fragmentation was not observed in the emulsion chamber experiment and therefore, for comparison with our results the ν-values have been averaged over the whole nucleus, i.e. $\bar{\nu}_A = \sum\pi_A(\nu)\cdot\nu$. The multiplicities in p-Al, p-Cu, p-Sn and p-W reactions are very close to the multiplicities given by eq. (10) for $\bar{\nu}(N_g) = \bar{\nu}_A$ (c.f. Fig. 11). This consistency among the observation in different kinds of experiments strongly supports the assumption that the quantity $\bar{\nu}(N_g)$ actually is a measure of the number of collisions between the incident hadron and the target nucleons.

5. Pseudo-rapidity distributions.

The total inclusive shower-particle spectrum in pseudo-rapidity is shown in Fig. 12 for different energies. The most striking feature observed here is the energy independence for small ($\eta \lesssim 1$) pseudo-rapidity values.

The energy independence of the shower particle multiplicities in the projectile fragmentation region is shown in Fig. 13. The rapidity variable, η', used in Fig. 13.

$$\eta' = \eta - \ln\left(\frac{s}{m^2}\right) \tag{11}$$

is an approximation to the projectile rest frame pseudo-rapidity. s is the square of the centre of mass energy and m is the nucleon mass. The independence is observed in the range $\eta' \geq -2$.

In Fig. 14 the distributions in the variable:

$$\eta'' = \eta \ln \frac{\sqrt{s}\langle\mu_\perp\rangle}{2m\langle p_\perp\rangle} \tag{12}$$

are exhibited. $\langle\mu_\perp\rangle$ is the transverse mass $\mu_\perp = \sqrt{p^2_\perp + m^2_\pi}$. The variable η'' is an approximation to the CMS-rapidity.

Apart from the two fragmentation regions there is a central part in the shower particle spectra. In ref. [10] the central region of pseudo-rapidity space was defined as

$$1 \leq \eta \leq \ln\left(\frac{s}{m^2}\right) - 2 \tag{13}$$

This was obtained by subtracting the energy independent target and projectile fragmentation parts. It can be seen from Fig. 13 that the total inclusive distribution rises with energy in this region.

It is of evident interest to consider the relationship between

shower particle multiplicities in the central region and the amount of nuclear matter passed by the incident hadron (N_h is a measure of this). Fig. 15 shows that the multiplicity density

$$\frac{\Delta n_s}{\Delta \eta} = \frac{n_s(\text{central region})}{\Delta \eta} \tag{14}$$

depends linearily on N_h and is energy independent in the range 200-400 GeV.

The shower particle multiplicity can then be evaluated in three different parts:

$$\begin{aligned} n_s(A,E) &= n_s^T(\text{target fragmentation}) + n_s^C(\text{central region}) + \\ &\quad + n_s^P(\text{projectile fragmentation}) \\ &= n_s^T(A) + n_s^C(A,E) + n_s^P \end{aligned} \tag{15}$$

The multiplicity in the central region, n_s^C, depends on energy, while the target and projectile fragmentation multiplicities, n_s^T and n_s^P, are energy independent. The multiplicities in the central region and the target fragmentation region are furthermore mass-dependent. A small decrease with increasing amount of traversed nuclear matter is observed in the very forward direction (i.e. for high rapidity values) [28] but this effect has been neglected here.

It has been pointed out in ref. [10] that the contribution from the fragmentation regions is so large at present energies that the energy independent features of the central region would be difficult to disentangle without a subtraction of this multiplicity.

It is therefore appropriate to study the energy dependent part

of the multiplicities by estimating ratios like:

$$r(E_1,E_2) = \frac{\langle n_s(E_1)\rangle - \langle n_s(E_2)\rangle}{\langle n_{ch}(E_1) - \langle n_{ch}(E_2)\rangle} \qquad (16)$$

r is a quantity where the energy independent contributions from the fragmentation regions have been subtracted, and corresponds roughly to the ratio of the central multiplicities in p-Em and pp-reactions.

Fig. 16 shows that r(E,200) is essentially energy independent for proton-emulsion nucleus collisions.

6. The height of the central plateau in p-A reactions.

The ratio $r'(\nu,E) = \frac{\langle n_s^C(A,E)\rangle}{\langle n_{ch}^C(H,E)\rangle}$ measures essentially the ratio of the central plateau in h-A reactions to that in pp-reactions. $n_s^C(A,E)$ and $n_{ch}^C(H,E)$ are the multiplicities in the central region in p-A and p-H reactions respectively. The width of the rapidity range in the central region, $\Delta\eta$, is, according to our partition above,

$$\Delta\eta = \ln\left(\frac{s}{m^2}\right) - 3 \qquad (17)$$

r' as a function of $\bar{\nu}(N_g)$ is shown in Fig. 17 for p-Em reactions at 400 GeV. The results exhibit a linear behaviour. Thus the multiplicity in the central region in p-A reactions at 400 GeV increases as

$$\langle n_s^C\ (Em,E,\nu)\rangle = \langle n_{ch}^C(H,E)\rangle\ (a+b(\bar{\nu}-1))$$

with the values a = 1.07 ± 0.11 and b = 0.83 ± 0.04.

$\langle n_s^C\rangle$ is the only energy dependent part of the multiplicity. Other multiplicity variables i.e. R or R_{eq} are of minor importance for studies of the energy dependence of shower particle

multiplicities, because they include the energy independent multiplicities from the projectile and target fragmentation regions.

Conclusions.

We observe that the main features of the 200-400 GeV data are very similar. In particular we conclude that:

i) The angular distribution of recoiling protons (grey track particles, N_g) is independent of energy and the identity of the impinging hadron.

ii) The correlation between $\langle N_b \rangle$ and N_g is independent of energy and the identity of the incident hadron.

iii) The scaled shower particle distributions differ slightly from the scaled distribution computed from the pp-distribution and summed over the target constituents.

iv) The incoherent shower particle multiplicity, $\langle n_s \rangle_i$, is larger than $\langle n_{ch} \rangle (0.5+0.5\langle \nu \rangle)$ and $\langle n_{ch} \rangle A^{0.14}$ at 400 GeV.

v) The average number of shower particles produced in each of the collisions inside the nucleus, $\langle n_1 \rangle$, seems to be independent of the nature of the incident hadron.

vi) $\bar{\nu}(N_g)$ provides a measure of the number of collisions inside the nucleus.

vii) It is of evident necessity to divide the rapidity space into three regions, the target fragmentation region, the central region and the projectile fragmentation region. The central region contains all the energy dependence. The target fragmentation depends only on the target mass while the projectile fragmentation region is essentially mass independent.

Acknowledgments.

We wish to express our gratitude to Dr. J. Sanford and Dr. L. Voyvodic of the Fermi National Accelerator Laboratory for their valuable help and cooperation during the planning of the experiment and the exposure of the stacks. We should also like to thank the supporting staff of the Fermi National Accelerator Laboratory for their assistance. Thanks are due to Dr. J. Babecki and Dr. R. Holyński for making available to us the experimental data concerning p-Em interactions at 67 and 200 GeV and π-Em interactions at 200 GeV. The financial help from the Swedish Natural Science Research Council is gratefully acknowledged.

Table 1. Shower particle multiplicities at different energies.

	Ref.	$\langle n_s \rangle$	$\langle n_{ch} \rangle [1+\frac{1}{2}(\langle \nu \rangle -1)]$	$\langle n_{ch} \rangle A^{.14}$	$\langle n_{ch} \rangle A^{.19}$
6.2 GeV	[1]	2.80 ± 0.04	5.2	5.2	6.4
22.5 GeV	[1]	5.61 ± 0.11	7.3	7.4	9.1
67 GeV	[20]	9.3 ± 0.2	10.2	10.3	12.6
200 GeV	[14]	13.2 ± 0.2	13.5	13.6	16.7
300 GeV	[15]	15.1 ± 0.2	15.0	15.0	18.5
400 GeV	This work	16.8 ± 0.4	15.8	15.9	19.6

References.

1. H. Winzeler, Nucl. Phys. 69 (1965) 661.

2. Z.V. Anzon et al. (Alma Ata-Leningrad-Moscow-Tashkent collaboration). Preprint 9 (1974).

3. Z.V. Anzon et al. (Alma Ata-Gatchina-Moscow-Tashkent collaboration). Preprint (1977).

4. J. Babecki et al., Phys. Lett. 47B (1973) 268 and private communication.

5. J. Babecki and G. Nowak, Krakow Report No 970/PH (1977), B. Furmańska et al., Krakow Report No 977/PH (1977).

6. Tsai-Chü et al. (Belgrade-Nancy-Lund-Lyon-Paris-Santander-Valencia collaboration). Lett. al Nuovo Cimento 20 (1977) 257.

7. B. Andersson, I. Otterlund and E. Stenlund, Phys. Lett. 73B (1978) 343.

8. K. Gottfried, Phys. Rev. Lett. 32 (1974) 957.

9. L. Bertocci, AIP Conference Proceedings 26 (1975) 238 (and references therein).

10. B. Andersson, G. Nilsson and I. Otterlund, Lund University Preprint LUTP-77-16 (1977) to be published.

11. Aggarwal et al., Nucl. Phys. B131 (1977) 61.

12. F. Fumuro et al., Proceedings of the 15th Int. Cosmic Ray Conf., Plovdiv, Bulgaria, Vol. 7 (1977) 59.

13. I. Otterlund et al. (Batavia-Belgrade-Lund-Lyon-Montreal-Nancy-Ottawa-Paris-Santander-Valencia collaboration). Proceedings of the 15th Int. Cosmic Ray Conf., Plovdiv, Bulgaria, Vol. 7 (1977) 40.

14. J. Hebert et al. (Barcelona-Batavia-Belgrade-Bucharest-Lund-Lyon-Montreal-Nancy-Ottawa-Paris-Rome-Strasbourg-Valencia collaboration). Phys. Lett. 48B (1974) 467.

15. J. Hebert et al. (Batavia-Belgrade-Lund-Lyon-Montreal-Nancy-Ottawa-Paris-Rome-Strasbourg-Valencia collaboration). Phys. Rev. D15 (1977) 1867.

16. A.A. Goryachikh, Zh. S. Takibaev, N.S. Titova and E.V. Shalagina, Sov. J. Nucl. Phys. 13 (1971) 729 (and references therein).

17. V.S. Barashenkov et al. Nucl. Phys. 14 (1959/60) 522.

18. R. Beaujean and H. Röhrs, Z. Physik 228 (1969) 308.

19. J. Babecki, private communications.

20. J. Babecki et al., Krakow Report No 929/PH (1976).

21. The conditions of this Monte Carlo calculation, where a flux of protons strikes nucleons in randomly generated nuclei, are the same conditions that must be fulfilled, if the expression $\langle\nu\rangle = \frac{A \cdot \sigma_{pp,inel}}{\sigma_{pA,inel}}$ is to be valid. The calculation is performed by the group in Lund.

22. P. Slattery, Phys. Rev. Lett. 29 (1972) 1624.

23. G. Calluci, R. Jengo and A. Pignolli, Phys.Rev. D10 (1974) 1468

24. A. Dar and J. Vary, Phys. Rev. D6 (1972) 2412.
E.M. Friedländer, Lett. al Nuovo Cimento 9 (1974) 349.
P.M. Fishbane, J. Vary, Phys. Lett. 51B (1974) 139.

25. J.M. Kohli, Nucl. Phys. B14 (1969) 500.

26. S.A. Azimov et al., Paper submitted to the Topical Meeting on Nuclear Production at Very High Energies, Trieste, June 1976 (and references therein).

27. C. Bromberg et al., Phys. Rev. Lett. 31 (1973) 1563.

28. B. Andersson and I. Otterlund, Nucl. Phys. B102 (1976) 238.
Alma Ata-Leningrad-Moscow-Tashkent collaboration, Sov. J. Nucl. Phys. 19 (1974) 536.
G. Fuijoka et al., Proceedings of the 15th Int. Cosmic Ray Conf., Plovdiv, Bulgaria, Vol. 7 (1977) 52.

Figure captions.

Fig. 1. The integral multiplicity distributions of heavy track producing particles. The line is fitted to 200 GeV data for $N_h \geq 8$. The data are from the following references: 200 GeV [2,4,14], 300 GeV [15] and 400 GeV [this work].

Fig. 2. The angular distribution of grey track producing particles (2.26 GeV [16], 6.2 GeV [1], 9 GeV [17], 19.5 GeV [16], 19.8 GeV [18], 22.5 GeV [1] 300-400 GeV [6] and 60 GeV (π-A) [16]).

Fig. 3. The mean number of black track producing particles as a function of the number of grey track particles (6.2 GeV [1], 22.5 GeV [1], 67 GeV [19], 200 GeV (p-A)[2], 400 GeV [this work] and 200 GeV (π-A)[19]).

Fig. 4. The grey particle multiplicity distribution at different energies, compared to predictions from eq. (3) (dashed line), 22.5 GeV [1], 200 GeV [4] and 400 GeV [this work].

Fig. 5. Scaled shower-particle distributions (67 GeV [19], 200 GeV [4,14], 300 GeV [15] and 400 GeV [this work]. The dashed curve is the scaled distribution computed from the Slattery curve [22] by using the experimental values obtained for $\langle n_s \rangle$ for collisions with hydrogen, light nuclei (CNO) and heavy nuclei (AgBr) of emulsion.

Fig. 6. The mean normalized shower particle multiplicity as a function of the number of heavy track particles. (200 GeV [2,4,14], 300 GeV [15] and 400 GeV [this work]).

Fig. 7. The mean number of heavy track particles as a function of the normalized multiplicity (200 GeV [2,4,13]), 300 GeV [13] and 400 GeV [this work]).

Fig. 8. $\langle n_s \rangle / D$ as a function of N_h (200 GeV [14], 300 GeV [13] and 400 GeV [this work]).

Fig. 9. $\langle n_1 \rangle = (\langle n_s \rangle_i - 0.5 \langle n_{ch} \rangle) \langle \nu \rangle^{-1}$ as a function of energy The curve corresponds to $\langle n_1 \rangle = \frac{1}{2} \langle n_{ch} \rangle$. The data are from references [1,11,14,15,19,20,25 and 26].

Fig. 10. The mean number of shower-particles as a function of the number of grey track-particles.

Fig. 11. The mean number of shower particles as a function of $\bar{\nu}(N_g)$ defined by eq. (5). The multiplicity in pp-reactions is from ref. [27] and the multiplicities in p-Al, p-Cu, p-Sn and p-W from ref. [12].

Fig. 12. The total inclusive shower-particle pseudo-rapidity distribution in the target nucleus rest frame.

Fig. 13. The total inclusive shower-particle distribution in the projectile rest frame.

Fig. 14. The total inclusive shower-particle distribution in the approximative nucleon-nucleon CMS.

Fig. 15. The density of shower-particles in the central region as a function of N_h.

Fig. 16. $r\ (E_1, 200) = (\langle n_s(E_1) \rangle - \langle n_s(200) \rangle)(\langle n_{ch}(E_1) \rangle - \langle n_{ch}(200) \rangle)^{-1}$ as a function of the incident proton energy.

Fig. 17. $r'(\bar{\nu},400) = \langle(n_s^C)\rangle\langle(n_{ch}^C)\rangle^{-1}$ as a function of $\bar{\nu}(N_g)$ obtained from p-Em reactions at 400 GeV.

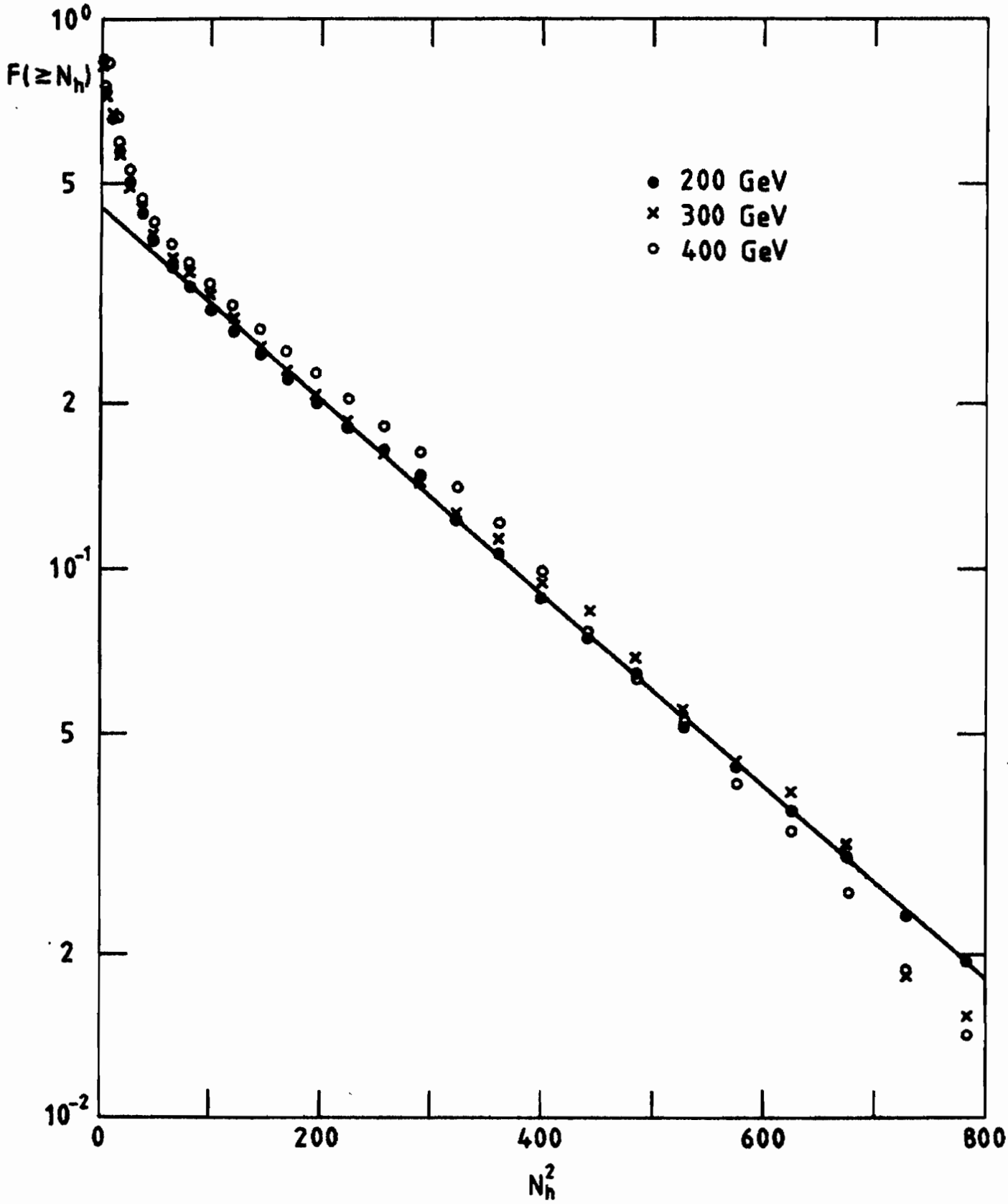
10^0
$F(\geq N_h)$
5
2
10^{-1}
5
2
10^{-2}
0
200
400
600
800
N_h^2
● 200 GeV
× 300 GeV
○ 400 GeV

Fig 1

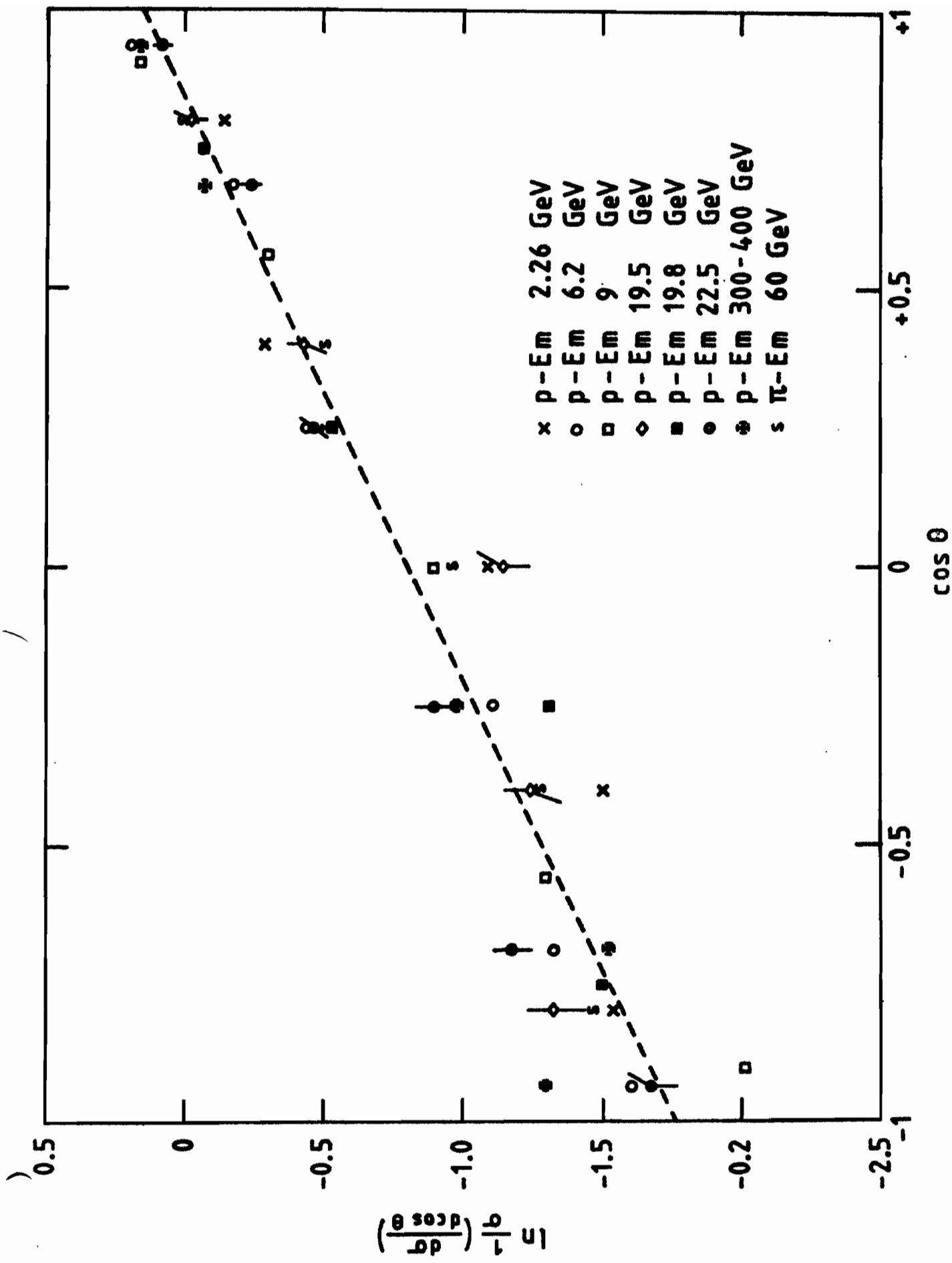
× p-Em 2.26 GeV
o p-Em 6.2 GeV
□ p-Em 9 GeV
◇ p-Em 19.5 GeV
■ p-Em 19.8 GeV
● p-Em 22.5 GeV
✱ p-Em 300-400 GeV
s π-Em 60 GeV
cos θ
ln 1/σ (dσ/dcos θ)
0.5
0
-0.5
-1.0
-1.5
-0.2
-2.5
-1
-0.5
0
+0.5
+1

Fig. 2

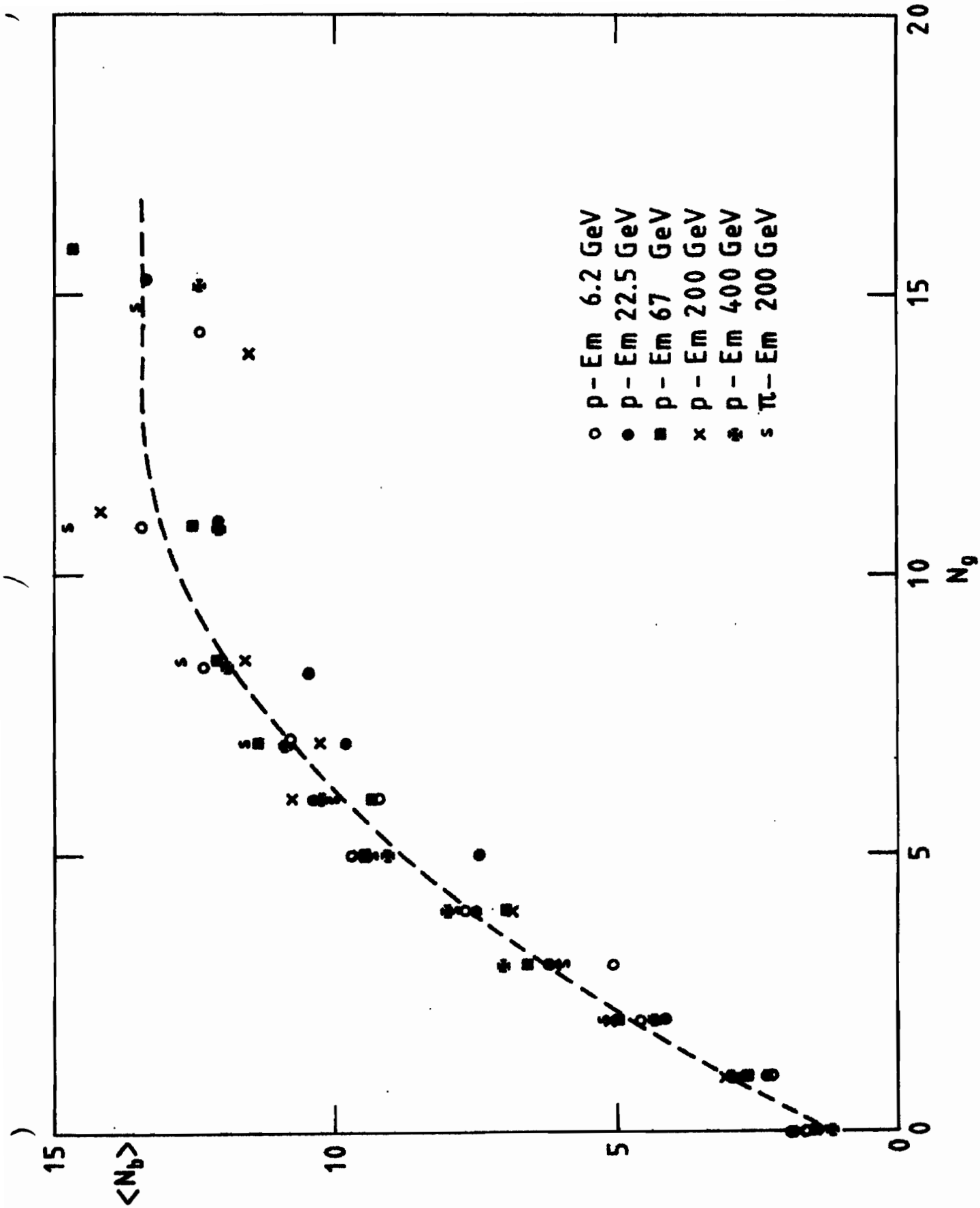
o p – Em 6.2 GeV
● p – Em 22.5 GeV
■ p – Em 67 GeV
x p – Em 200 GeV
* p – Em 400 GeV
s π– Em 200 GeV
<N_b>
N_g
0
5
10
15
20

Fig. 3

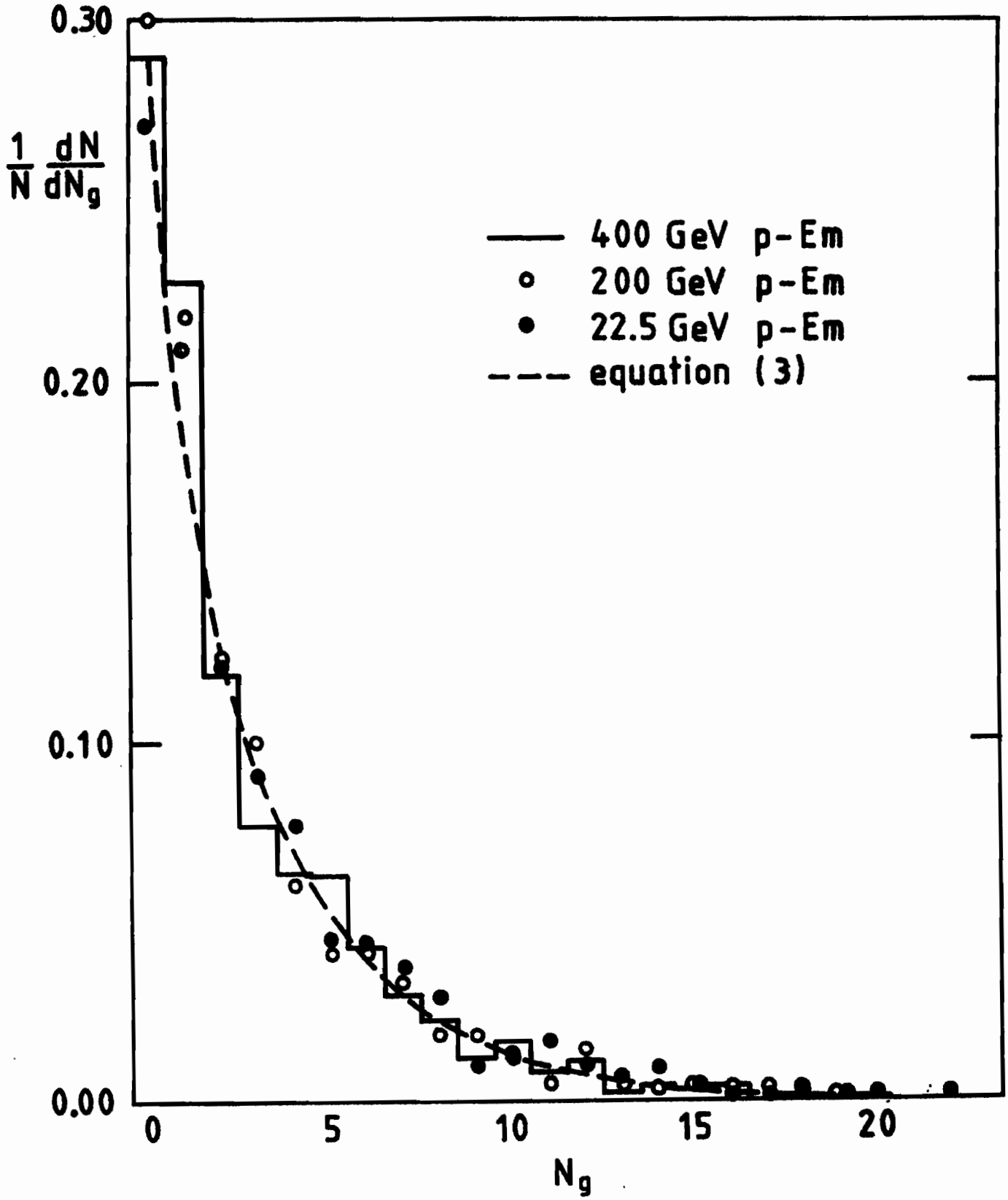
0.30
0.20
0.10
0.00
$\frac{1}{N}\frac{dN}{dN_g}$
400 GeV p-Em
200 GeV p-Em
22.5 GeV p-Em
equation (3)
0
5
10
15
20
N_g

Fig. 4

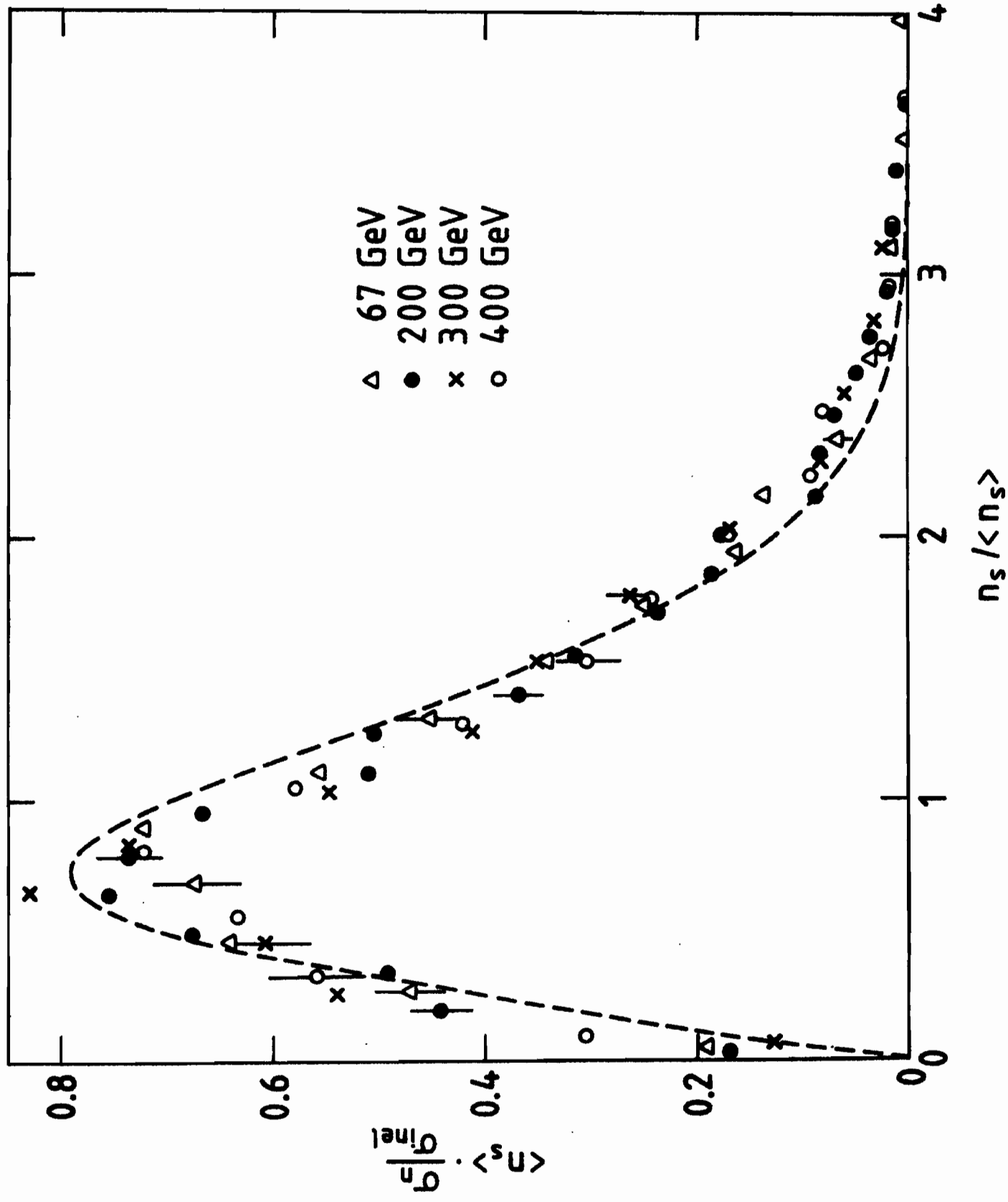
67 GeV
200 GeV
300 GeV
400 GeV
$\langle n_s \rangle \cdot \frac{\sigma_n}{\sigma_{inel}}$
$n_s / \langle n_s \rangle$
0.8
0.6
0.4
0.2
0
0
1
2
3
4

Fig.5

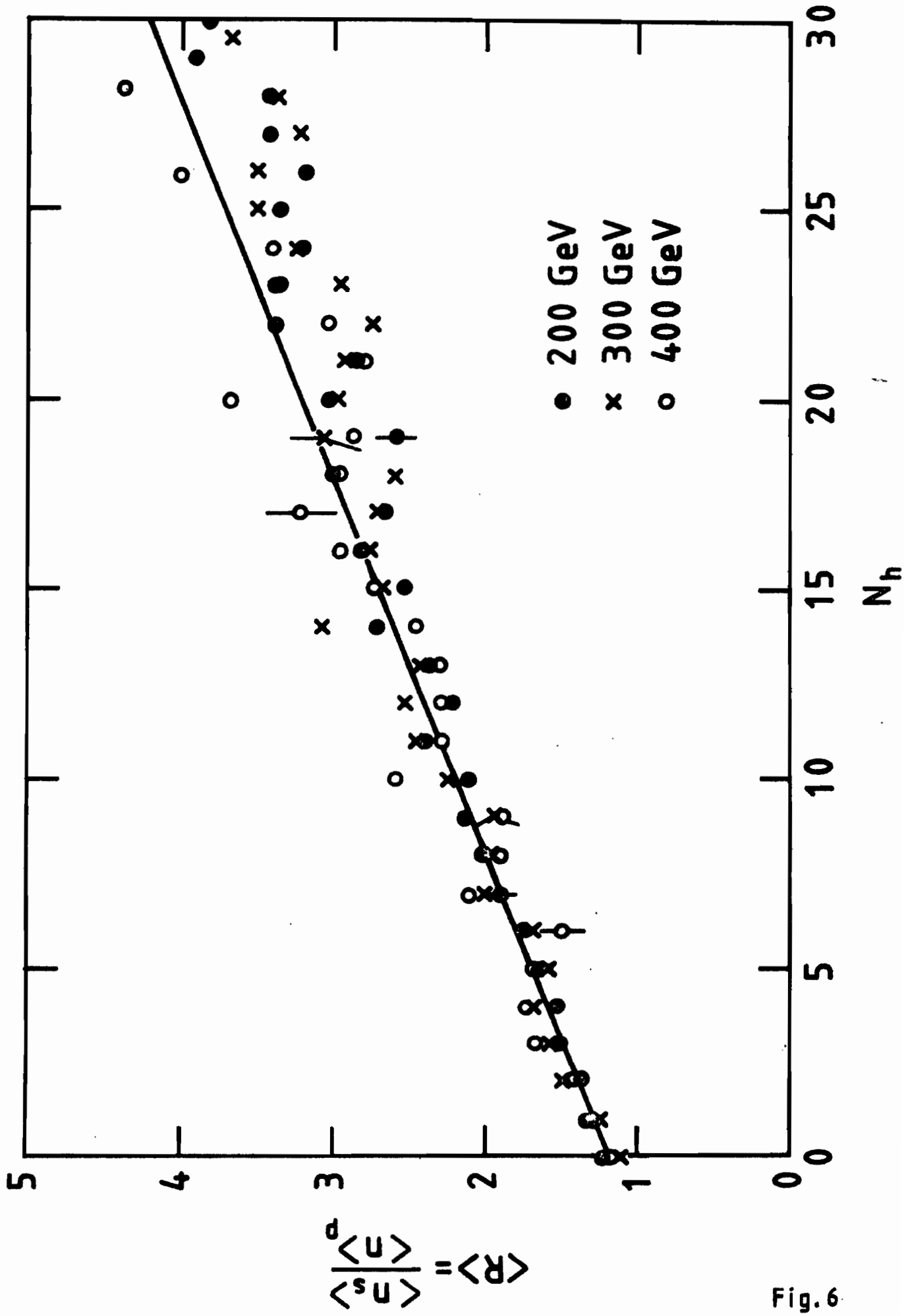
200 GeV
300 GeV
400 GeV
N_h
$\langle R \rangle = \frac{\langle n_s \rangle}{\langle n \rangle_p}$
0
5
10
15
20
25
30
1
2
3
4
5

Fig. 6

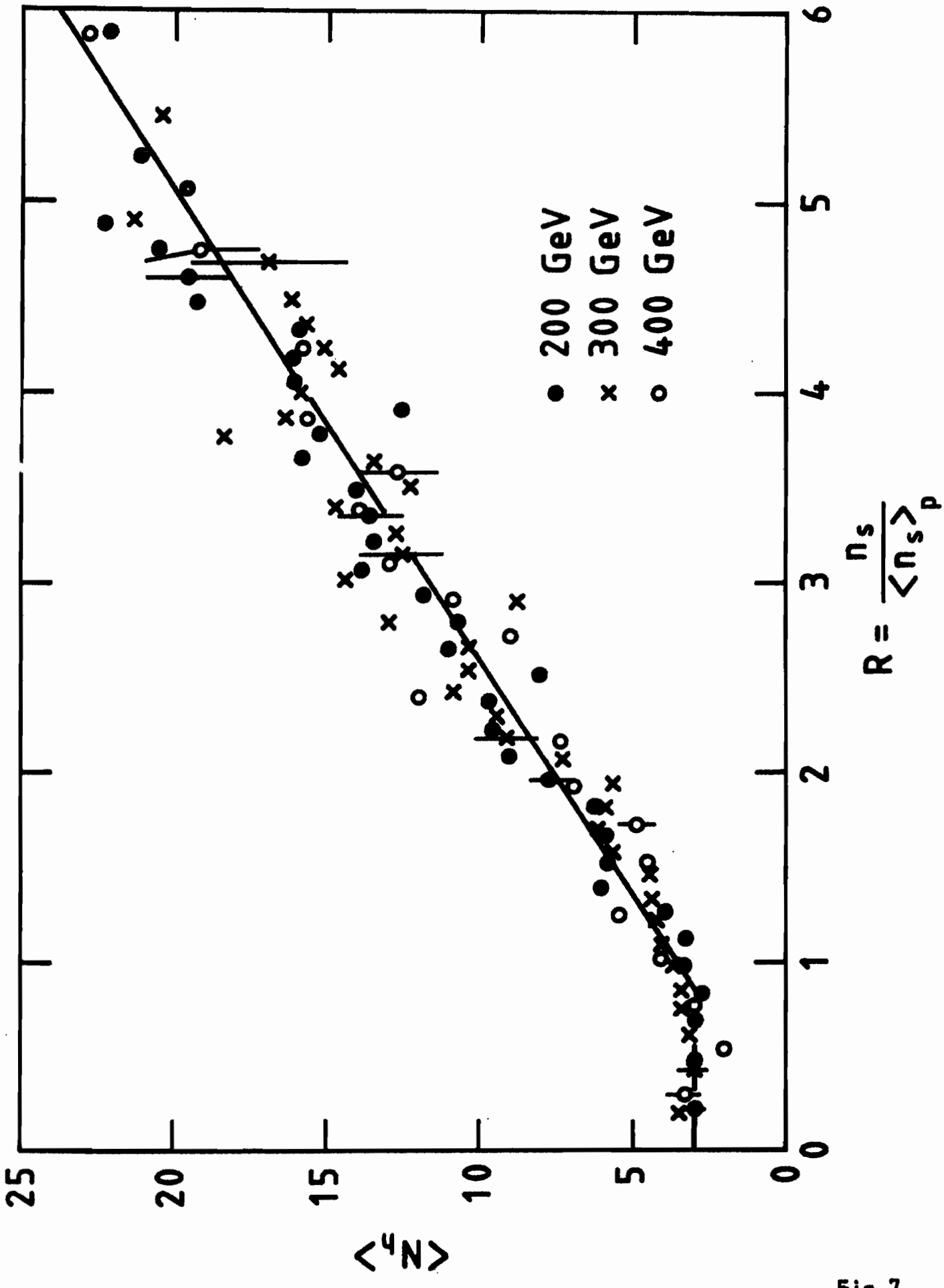
200 GeV
300 GeV
400 GeV
$R = \frac{n_s}{\langle n_s \rangle_p}$
$\langle N_4 \rangle$
0
5
10
15
20
25
1
2
3
4
5
6

Fig. 7

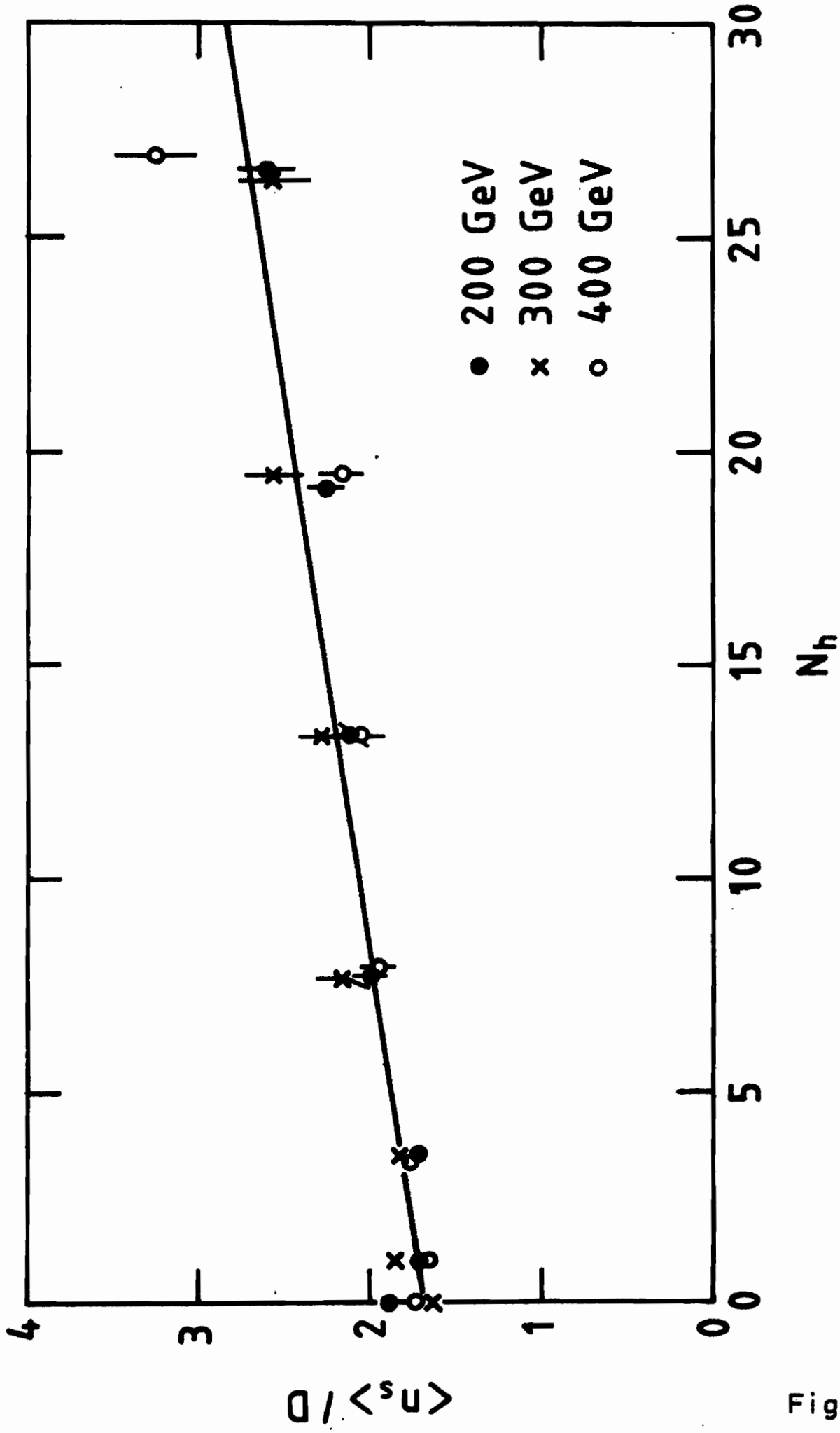
4
3
2
1
0
$\langle n_s \rangle / D$
0
5
10
15
20
25
30
N_h
● 200 GeV
× 300 GeV
○ 400 GeV

Fig.8

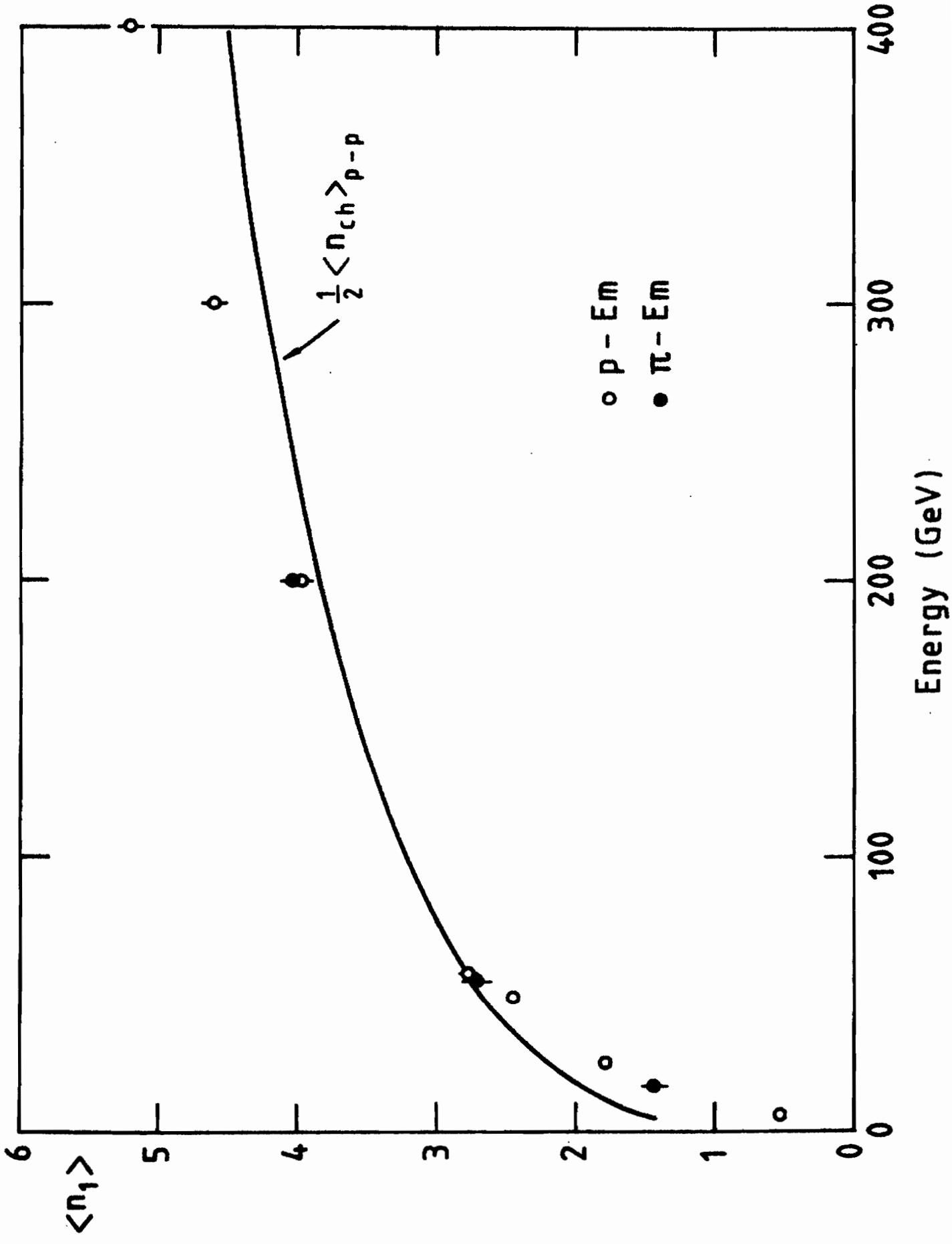
$\langle n_1 \rangle$
0
1
2
3
4
5
6
0
100
200
300
400
Energy (GeV)
$\frac{1}{2}\langle n_{ch} \rangle_{p-p}$
o p - Em
• π - Em

Fig. 9

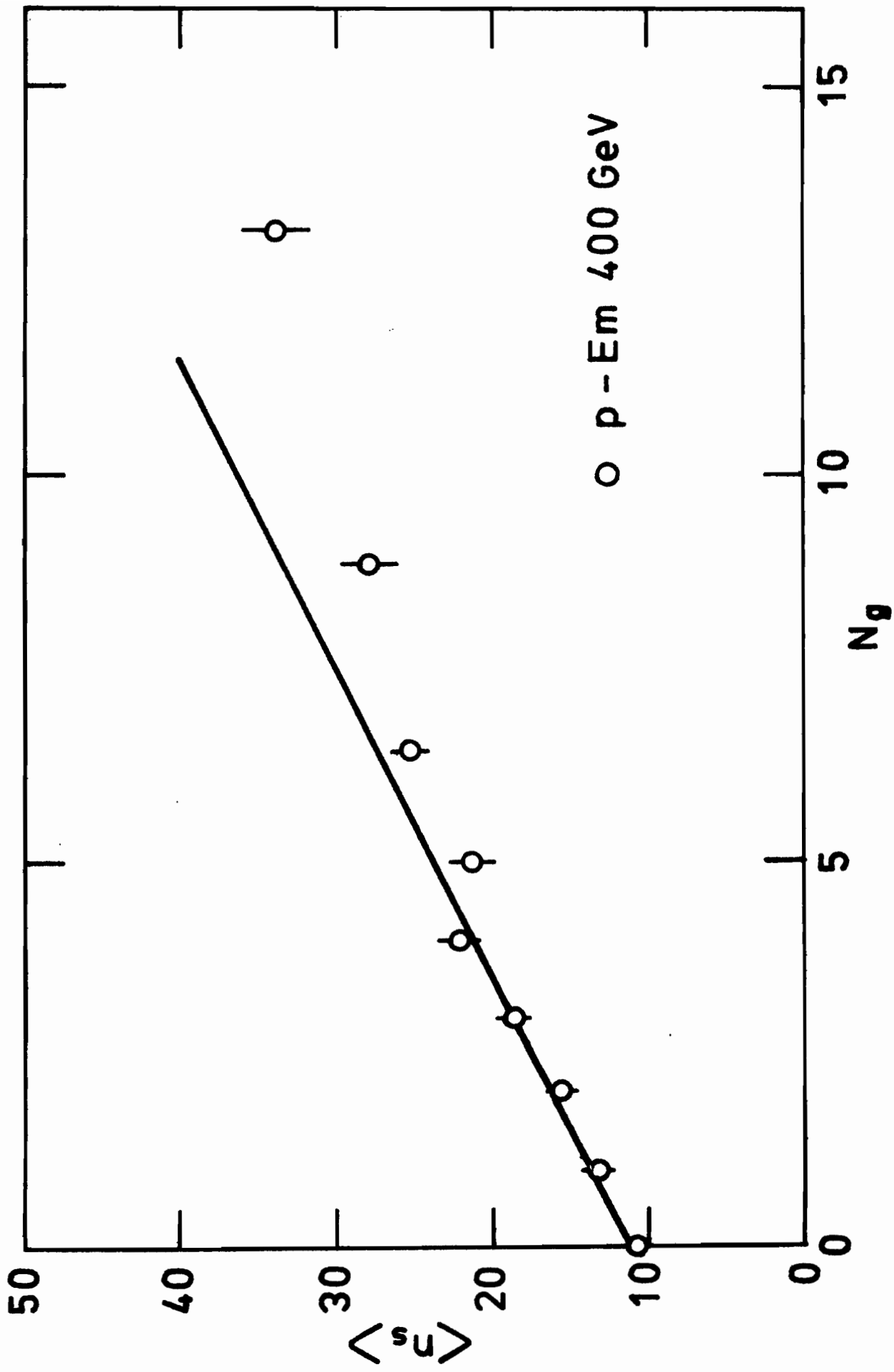

Fig. 10

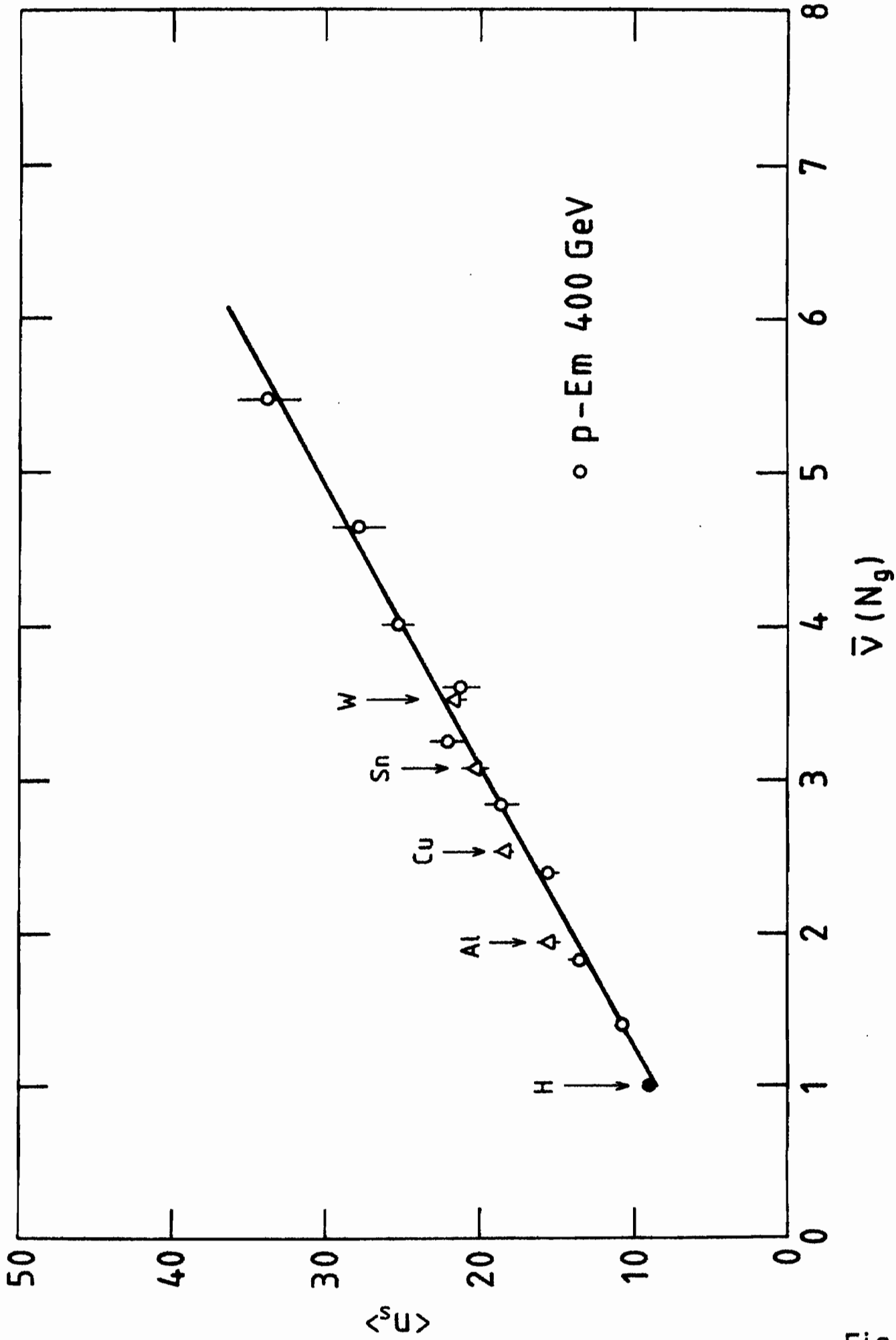

Fig. 11

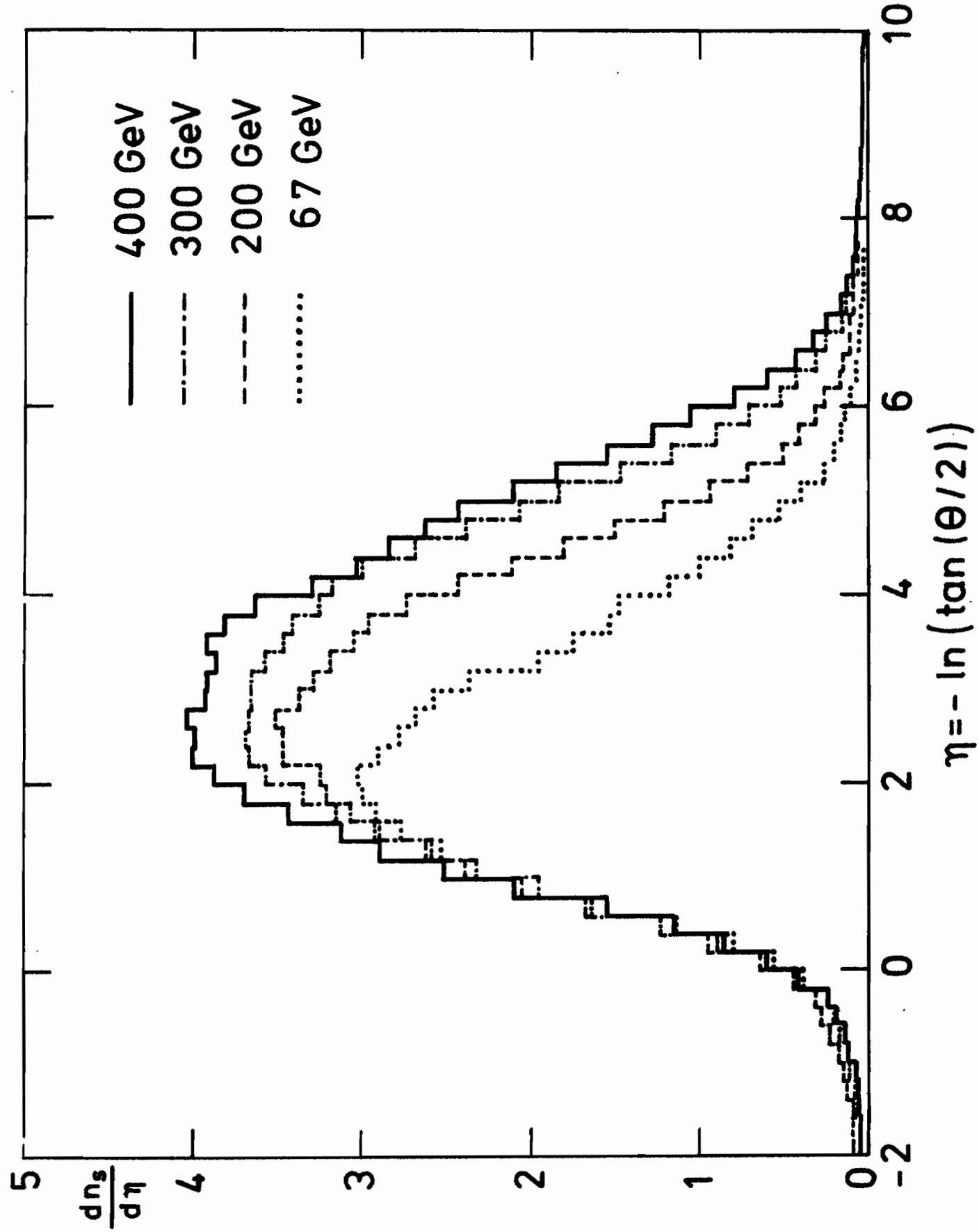
400 GeV
300 GeV
200 GeV
67 GeV
$\frac{dn_s}{d\eta}$
5
4
3
2
1
0
-2
0
2
4
6
8
10
$\eta = -\ln(\tan(\theta/2))$

Fig.12

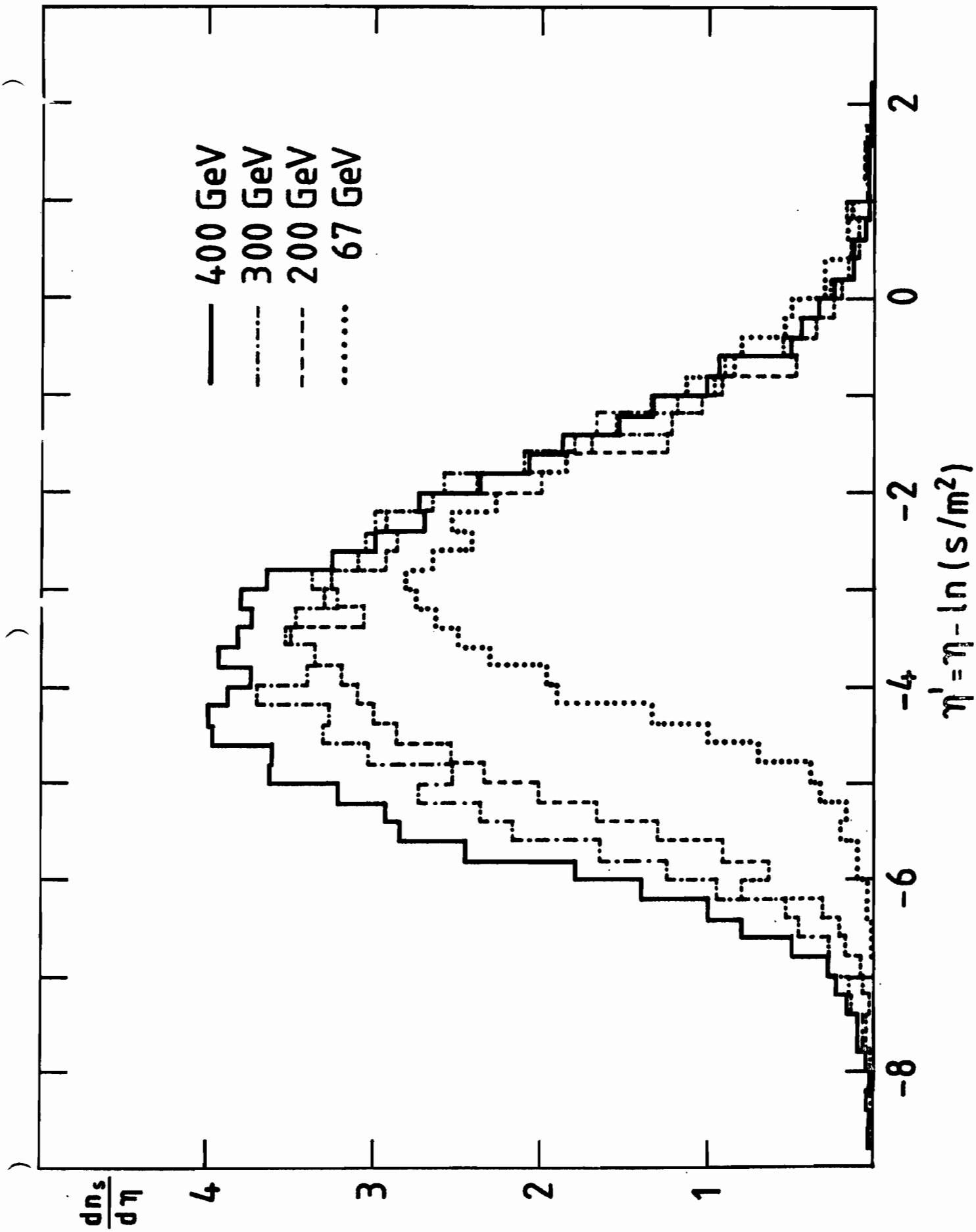
400 GeV
300 GeV
200 GeV
67 GeV
$\frac{dn_s}{d\eta}$
4
3
2
1
-8
-6
-4
-2
0
2
$\eta' = \eta - \ln(s/m^2)$

Fig.13

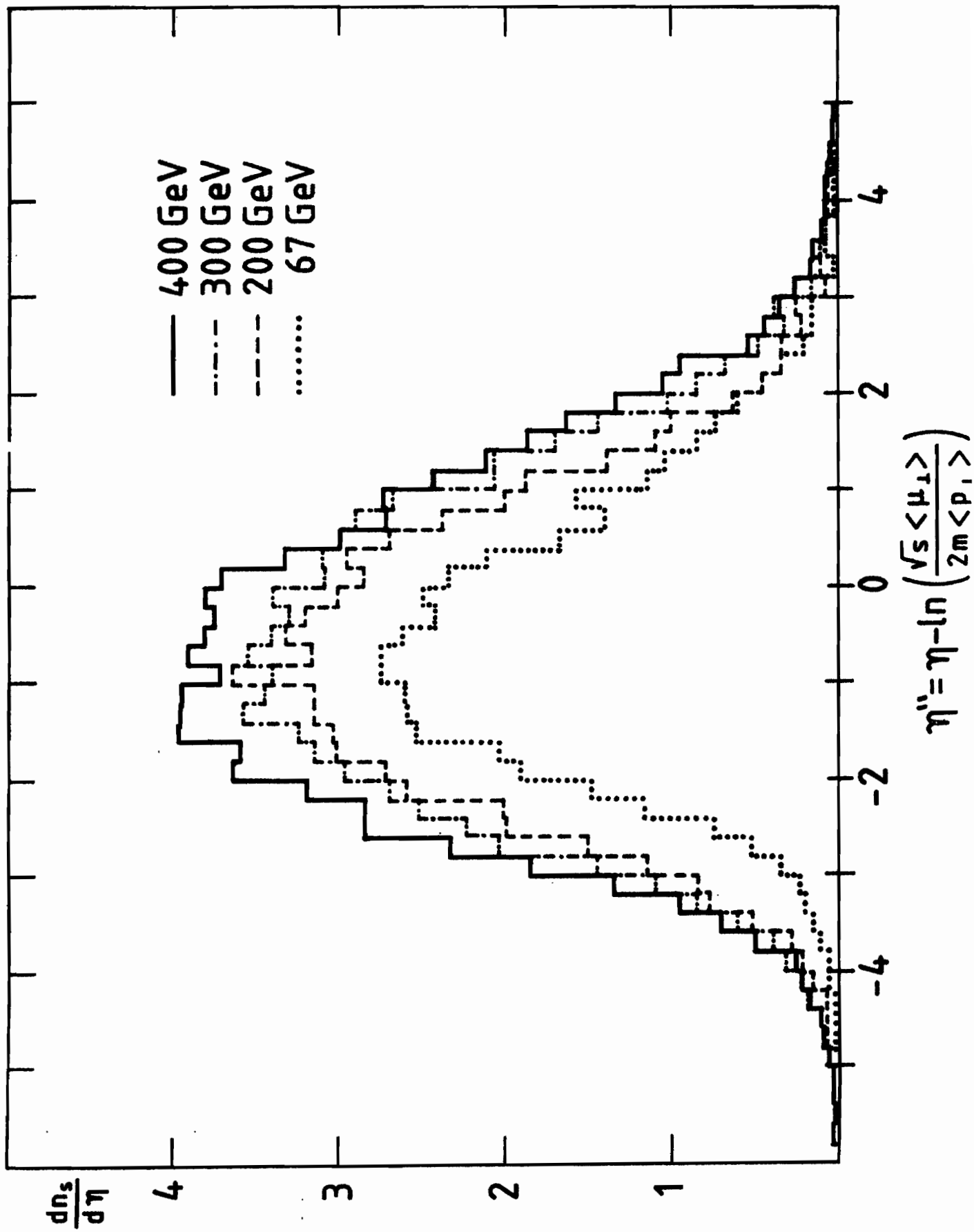
400 GeV
300 GeV
200 GeV
67 GeV
$\frac{dn_s}{d\eta}$
4
3
2
1
-4
-2
0
2
4
$\eta'' = \eta - \ln\left(\frac{\sqrt{s}\langle\mu_\perp\rangle}{2m\langle p_\perp\rangle}\right)$

Fig. 14

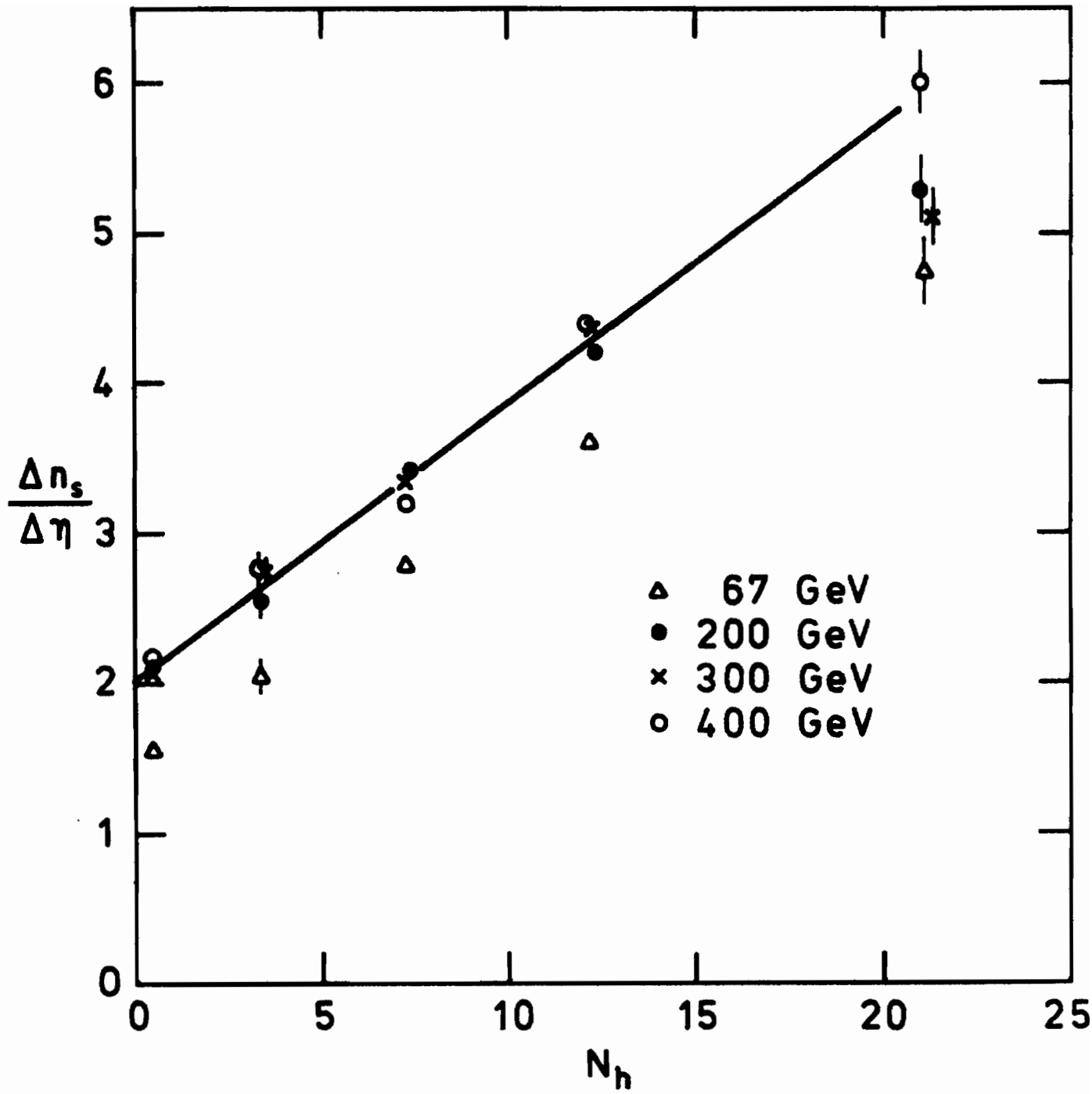
6
5
4
3
2
1
0
$\frac{\Delta n_s}{\Delta \eta}$
0
5
10
15
20
25
N_h
67 GeV
200 GeV
300 GeV
400 GeV

Fig. 15

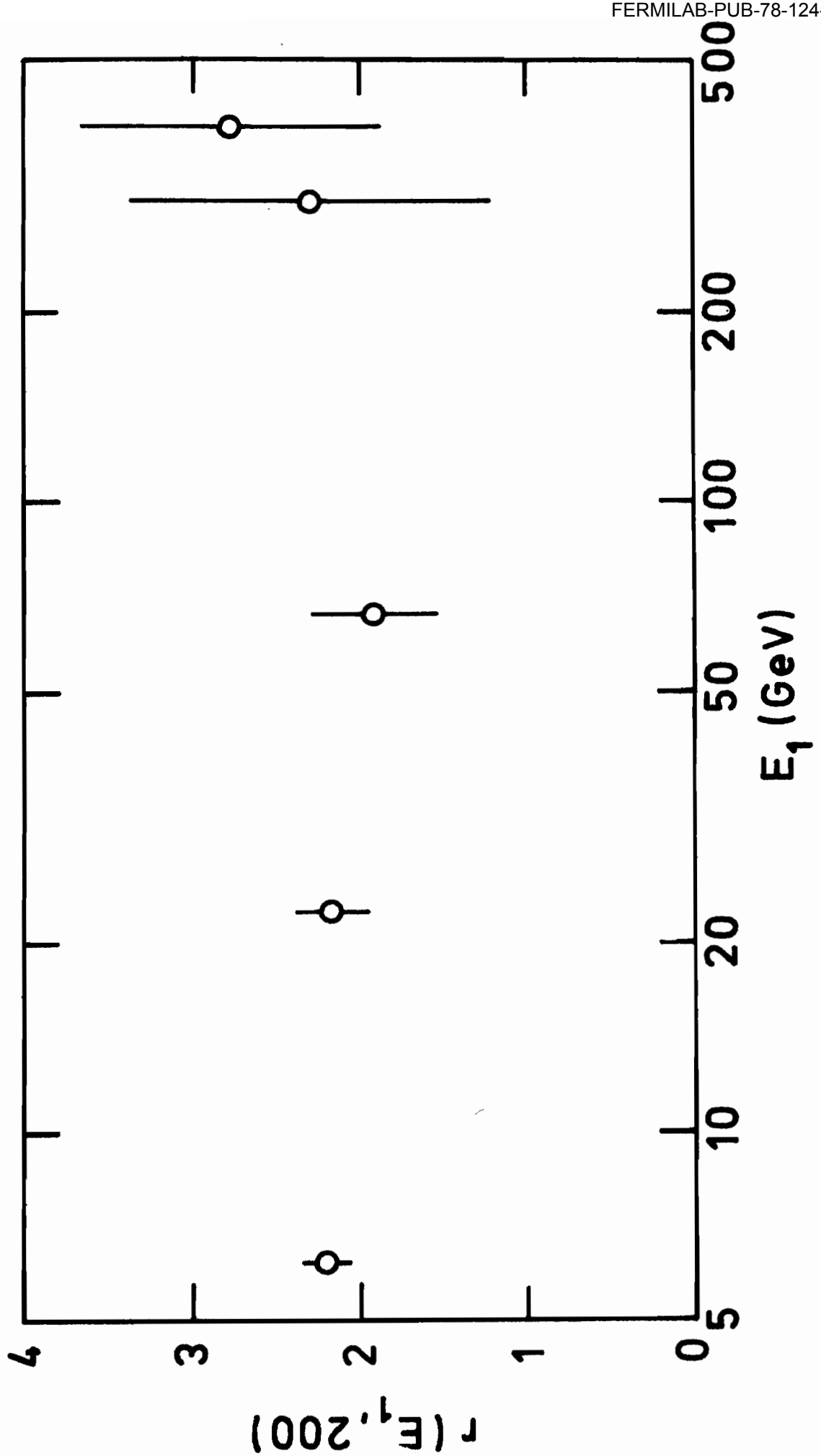

Fig.16

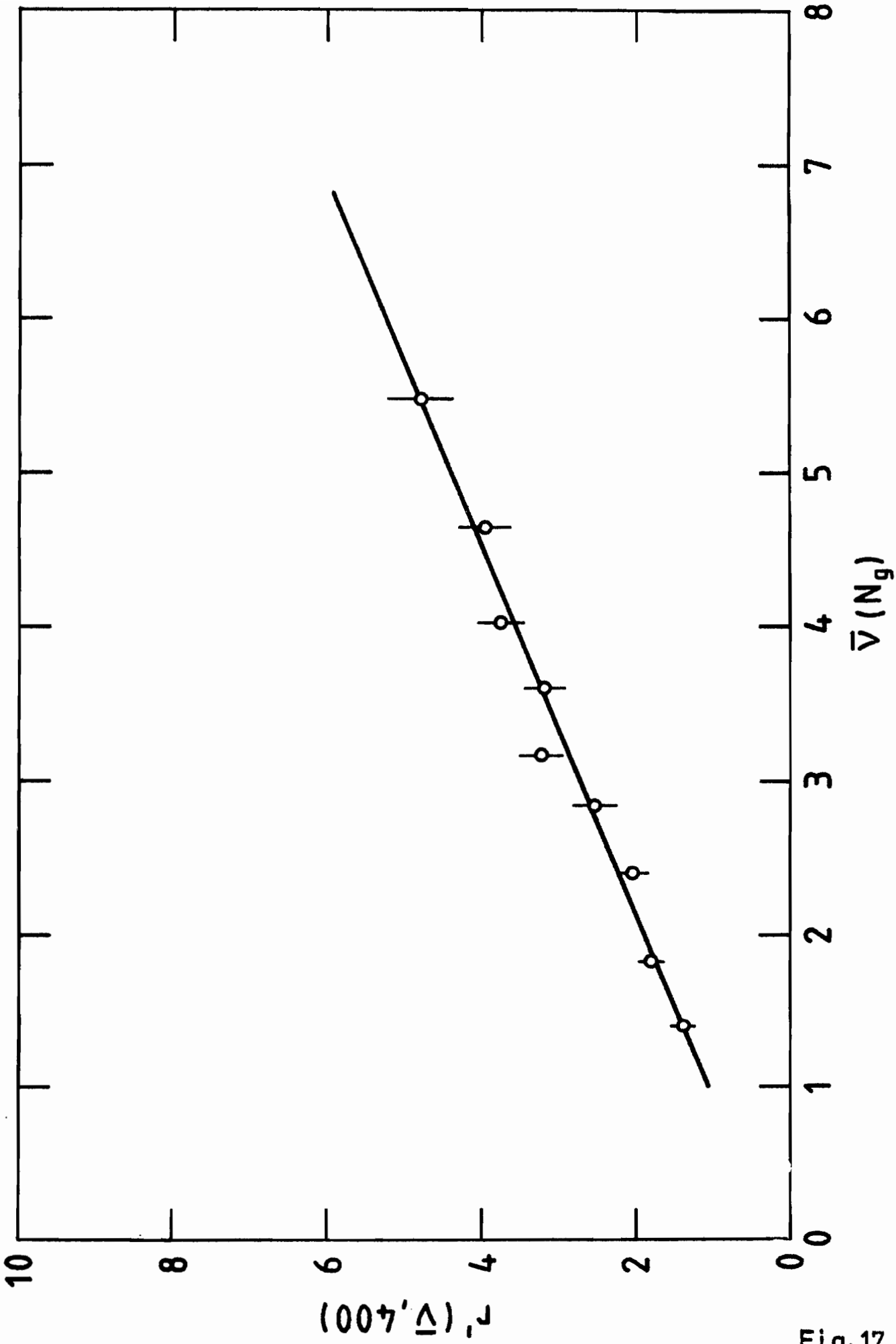

Fig. 17

FERMILAB-PUB-78-124-E

Dokumentutgivare
UNIVERSITY OF LUND
Handläggare Department of Physics

Dokumentnamn
Internal report
Utgivningsdatum
1978-04-13

Dokumentbeteckning
LUNFD6/(NFFK-7004)
Ärendebeteckning

Författare

I. Otterlund
E. Stenlund
et al.

Dokumenttitel och undertitel

Nuclear Interactions of 400 GeV Protons in Emulsion.

Referat (sammandrag)

We report on 400 GeV proton-emulsion nucleus reactions and compare the results to hadron-nucleus reactions at smaller energies. In particular we present results on the emission of fast target protons (essentially grey track particles) and on their correlation with the number of collisions inside the nucleus, ν, with the number of charged evaporated particles (essentially black track particles) and with the number of pions produced (essentially shower particles). We observe that the main features of the 200-400 GeV data are very similar. However, we find that the mean shower-particle multiplicity at 400 GeV is essentially higher than expected from the simple independent particle model prediction $\langle n_s \rangle = \langle n_{ch} \rangle [1 + 0.5 (\langle \nu \rangle - 1)]$. The shower particle multiplicities do not seem to follow a target mass dependence of the form $\langle n_s \rangle = \langle n_{ch} \rangle A^{\alpha}$ with $\alpha = 0.14$ or $\alpha = 0.19$ as has been suggested in the literature. The pseudo-rapidity distribution shows limiting target and projectile fragmentation. The shower particle multiplicity in the "central region" increases linearily with $\langle \nu \rangle$ but faster than 0.5 $\langle \nu \rangle$ times the corresponding multiplicity in pp-reactions.

Referat skrivet av
The editors

Förslag till ytterligare nyckelord

Klassifikationssystem och -klass(er)

Indextermer (ange källa)

Omfång 20 pages + 17 figures.

Övriga bibliografiska uppgifter

Språk

Sekretessuppgifter

ISSN

ISBN

Dokumentet kan erhållas från
Department of Cosmic and Subatomic Physics
University of Lund, Sölvegatan 14,
S-223 62 LUND, Sweden.

Mottagarens uppgifter

Pris

Blankett LU 11:25 1976-07